


Article

Recycling of Bulk Polyamide 6 by Dissolution-Precipitation in CaCl₂-EtOH-H₂O Mixtures

Ruben Goldhahn ¹, Ann-Joelle Minor ¹, Liisa Rihko-Struckmann ¹, Siew-Wan Ohl ², Patricia Pfeiffer ²,
Claus-Dieter Ohl ² and Kai Sundmacher ^{1,3,*}

¹ Max Planck Institute for Dynamics of Complex Technical Systems, Department of Process Systems Engineering, Sandtorstraße 1, 39106 Magdeburg, Germany

² Institute of Physics, Faculty of Natural Sciences, Otto-von-Guericke University, Universitätsplatz 2, 39106 Magdeburg, Germany

³ Institute of Process Engineering, Faculty of Process and Systems Engineering, Otto-von-Guericke University, Universitätsplatz 2, 39106 Magdeburg, Germany

* Correspondence: sundmacher@mpi-magdeburg.mpg.de; Tel.: +49-391-6110-351

Abstract: To address the problems of virgin plastic production from fossil resources and the growing amount of plastic waste, a rapid transition to a circular economy is being pursued. The separation of mixed plastics into pure fractions is of paramount importance for promoting recycling and preventing downcycling. In this study, experimental parameters were determined for the selective bulk dissolution of polyamide 6 (PA 6) filaments (1.75 mm diameter, 1 cm length) in CaCl₂-EtOH-H₂O mixtures (CEW) at 75 °C. These parameters included the energy supply mode, dissolution time, CEW composition and CEW:PA mass ratio. Compared with energy supply by microwaves, energy supply by ultrasound improved the yield of dissolved and recovered PA 6 after 5 h from 31% to 52%. In total, the yield of PA 6 after 3 h of bulk dissolution increased from 18% to 69% when the energy supply mode was changed from microwave to ultrasound and the H₂O:EtOH molar ratio of CEW was increased from 0.40 to 1.33 while maintaining an optimal CEW:PA mass ratio of 8.5. Additionally, master plot analysis suggested that dissolution under microwave energy supply followed a contracting cylinder model, whereas dissolution under ultrasonic energy supply aligned with a 2D diffusion or third-order kinetic model. Microscopic observations suggested that, in the case of ultrasonic energy supply, oscillating bubbles on the particle surface enhanced the dissolution rate of PA 6 filaments in CEW.

Keywords: circular economy; polymer recycling; polyamide 6; dissolution-reprecipitation; process intensification



Academic Editors: Grace Wan-Ting Chen, Daniel Lachos-Perez and Taofeng Lu

Received: 18 November 2024

Revised: 12 December 2024

Accepted: 20 December 2024

Published: 3 January 2025

Citation: Goldhahn, R.; Minor, A.-J.; Rihko-Struckmann, L.; Ohl, S.-W.; Pfeiffer, P.; Ohl, C.-D.; Sundmacher, K. Recycling of Bulk Polyamide 6 by Dissolution-Precipitation in CaCl₂-EtOH-H₂O Mixtures. *Recycling* **2025**, *10*, 5. <https://doi.org/10.3390/recycling10010005>

Copyright: © 2025 by the authors. Licensee MDPI, Basel, Switzerland. This article is an open access article distributed under the terms and conditions of the Creative Commons Attribution (CC BY) license (<https://creativecommons.org/licenses/by/4.0/>).

1. Introduction

Humanity must reduce the extraction of fossil resources as quickly as possible to limit anthropogenic climate change [1,2]. In addition, there is an urgent need for innovative solutions to reduce and manage plastic waste to combat the escalating global plastic waste crisis [3]. The concept of a circular economy, which aims to minimize waste generation and maximize resource efficiency, holds potential to address these two challenges [4]. Within the waste hierarchy framework, after refusing, rethinking, reducing, reusing, repurposing and repairing, plastic recycling plays a pivotal role by transforming waste plastics into valuable resources [5]. Because plastics are frequently recovered as mixed waste streams, before an effective recycling process can be initiated, a preliminary stage must separate different types of plastics into high-purity polymer fractions, thereby minimizing downcycling [6–9].

This study focuses on the polymer PA 6. PA 6 manufacturing is particularly resource intensive, making its production through recycling methods highly beneficial [10]. PA 6 can be recycled mechanically, physically, biologically, chemically or thermally [9,11–13]. Compared with other recycling technologies, physical dissolution-precipitation should be the least energy intensive [14–16] because only the hydrogen bonds between the polymer chains need to be disrupted; by contrast, chemical recycling requires covalent bonds to be broken. Therefore, we focus on the selective dissolution of PA 6 as a technique to separate PA 6 from other polymers. Selective dissolution involves multiple steps: dissolving only PA 6 from the mixture, separating the solution from the other polymers, and reprecipitating PA 6 from the solvent with the help of an antisolvent, as shown in Figure 1. Previous studies have selectively dissolved PA 6 in phenol and 3-methylphenol [17], formic acid [18–20], ethane-1,2-diol [21], dimethyl sulfoxide [22], tributyl(ethyl)phosphonium diethyl phosphate ($[P_{4442}][Et_2PO_4]$) [23] and $CaCl_2$ -EtOH- H_2O mixtures (CEW) [24]. Antisolvents used to precipitate the polymer chains include toluene [17,18], xylene [17], methanol [18], dimethylformamide [18], hexane [18], butan-2-one [18,19,22], dimethyl sulfoxide [18], and water [24–27].

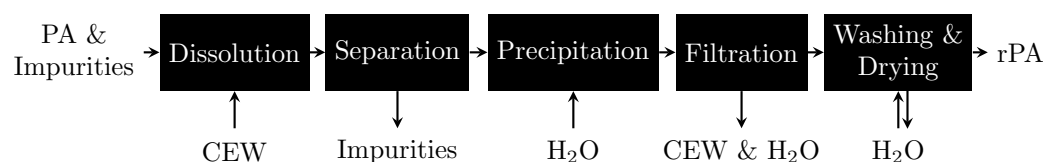


Figure 1. Scheme for selective PA 6 dissolution experiments with subsequent PA 6 recovery using CEW as the solvent and H_2O as the antisolvent.

The selective dissolution of PA 6 in CEW has several advantages: it does not alter the polymer's molecular weight distribution [24]; it uses low temperatures ($75\text{ }^\circ\text{C}$) [24] and non-toxic chemicals that are readily available (H_2O), can be bio-based (EtOH) and come as low-value side products from other large-scale processes ($CaCl_2$ is a waste product of the Solvay process to produce soda Na_2CO_3). Furthermore, the solvent CEW has been shown not to dissolve PET [24], PU [24], cotton [24] as well as wool [26] and can therefore be seen as a selective solvent for PA 6. This work presents the first instance of the dissolution of bulk PA 6 in CEW. The objective of this study was to experimentally investigate the operational parameters for the dissolution of bulk PA 6 in CEW to provide a scale-up concept for industrial application. These parameters included the energy supply mode, dissolution time, CEW composition and CEW:PA ratio. To ensure the quality of the results, the mass balances, conversions and recoveries of the dissolution experiments were determined. In addition, the Ca^{2+} content and molecular weight distribution of the recovered PA 6 were analyzed, and initial mechanistic investigations were conducted.

2. Materials and Methods

Figure 1 shows a schematic representation of the selective dissolution procedure for PA 6. The polymer sample used in this study was free of impurities such as additives and colorants. Each experiment was performed at least three times, and the results are presented as averages and relative sample standard deviations.

2.1. Materials and Equipment for Dissolution Experiments

Nylon PA 6 low-warp filament with a circular cross-section (1.75 mm diameter; Spectrum Filament) was cut into 1-cm-long pieces. Calcium chloride dihydrate ($CaCl_2 \cdot 2H_2O \geq 99\%$) and calcium chloride ($CaCl_2 97\%$) were procured from Sigma-Aldrich. Absolute ethanol (EtOH 99.9%) was purchased from Merck. All purchased materials were used as

received. Ultrapure water (H_2O resistivity $18.2 \text{ M}\Omega\cdot\text{cm}$) was prepared using a Milli Q IQ 7000 with a Millipak 0.22- μm filter.

A Bandelin Sonorex RK 106 (35 kHz) ultrasonic bath was employed for solvent formulation, and a Bandelin Sonorex RK 102 h (35 kHz) ultrasonic bath was used for the dissolution procedure. As indicated by the measurements presented in the Supplementary Information (S9), the acoustic pressure from peak to peak was 0.8 bar, and the main frequency was the driving frequency, accompanied by harmonics and subharmonics. A Discover 2.0 microwave synthesizer (CEM Corporation, 2.45 GHz) was employed for the microwave dissolution experiments. Whatman grade glass fiber filter papers (GF 92) were procured from Cytiva.

2.2. Solvent Formulation

The CEW mixtures were prepared by adding the weighed quantities of the three components to a 50-mL Erlenmeyer flask, which was then sealed and placed in an ultrasonic bath at $25 \text{ }^\circ\text{C}$. $\text{CaCl}_2\cdot 2\text{H}_2\text{O}$ was used for solvent compositions with $\frac{n(\text{CaCl}_2)}{n(\text{H}_2\text{O})} = \frac{1}{2}$; otherwise, anhydrous CaCl_2 and H_2O were added separately. In the case of separate addition, a slight yellow coloring of the solvent was observed. The applied compositions are noted in Table 1. After 30 min in the ultrasonic bath, the homogeneous solution was cooled in a water bath for 5 min, and depending on the desired mass ratio of CEW:PA, the appropriate amount (4–30 g) of CEW was mixed with $m_{\text{PA}} = 1 \text{ g}$ of the cut PA 6 filament in a 35-mL Pyrex pressure vessel (CEM Corporation) (or 100-mL pressure vessel in the case of CEW:PA ≥ 15). Note that the solubility of CaCl_2 in CEW is limited to $x_{\text{CaCl}_2} < 0.3$.

Table 1. Molar compositions of various CEW mixtures used in this work with a constant molar fraction of $x_{\text{CaCl}_2} = 0.125$.

CEW	$x_{\text{H}_2\text{O}}$	x_{EtOH}	$\text{H}_2\text{O}:\text{EtOH}$ Molar Ratio
A	0.000	0.875	0.00
B	0.125	0.750	0.17
C	0.250	0.625	0.40
D	0.375	0.500	0.75
E	0.500	0.375	1.33
F	0.625	0.250	2.50
G	0.750	0.125	6.00

2.3. Dissolution Procedure

The sealed vessel was placed in a preheated ultrasonic bath for the desired dissolution time at a constant temperature. Alternatively, a glass-coated stir bar was added, and the vessel was placed in a microwave chamber, where it was heated and stirred at 600 rpm for the dissolution time. The dissolution was conducted at $75 \text{ }^\circ\text{C}$, in line with Qianhui et al. (2023) [24]. After the desired dissolution time, the undissolved PA 6 filaments were carefully removed from the vessel using a spatula while leaving as much of the clear solution containing CEW and dissolved PA in the vessel as possible. The undissolved filaments were spread on preweighed filter paper (m_{F}) and washed on a vacuum filtration setup with 1000 mL of H_2O to remove all CaCl_2 . After washing, the filter paper with the residual undissolved filaments (uPA) was dried at $40 \text{ }^\circ\text{C}$ overnight and subsequently weighed ($m_{\text{F}+\text{uPA}}$) to determine the conversion according to Equation (1):

$$X_{\text{PA}}[\%] = \frac{m_{\text{PA}} - m_{\text{F}+\text{uPA}} - m_{\text{F}}}{m_{\text{PA}}} \cdot 100 = 1 - \frac{m_{\text{uPA}}}{m_{\text{PA}}} \cdot 100 \quad (1)$$

2.4. Recovery of PA 6

After separation from uPA, the PA 6 dissolved in CEW was recovered by the addition of H₂O as an antisolvent (AS). The mass ratio of added antisolvent was fixed to $\frac{m_{AS}}{m_{CEW}} = 2.35$. Following the addition of the antisolvent, the dissolved PA 6 precipitated from CEW, and the amorphous agglomerates gradually solidified. During solidification, the precipitated PA 6 was cut into small pieces ($\leq 2 \text{ mm}^3$), placed on preweighed filter paper, and washed with 1000 mL of H₂O on a vacuum filtration setup. The filter paper with the precipitated PA 6 (rPA) was dried at 40 °C overnight and weighed (m_{F+rPA}) to determine the yield of rPA according to Equation (2):

$$Y_{PA}[\%] = \frac{m_{F+rPA} - m_F}{m_{PA}} \cdot 100 = \frac{m_{rPA}}{m_{PA}} \cdot 100 \quad (2)$$

Figure 2 shows images of the precut PA 6 filaments, uPA, and rPA.

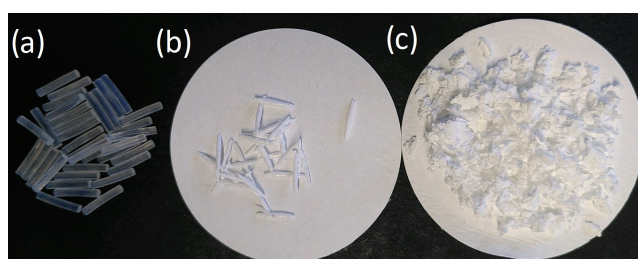


Figure 2. (a) 1 cm precut PA 6 filaments; (b) undissolved and washed PA 6 residue filaments; (c) recovered PA 6 after dissolution and precipitation.

The overall PA 6 mass balance was calculated using Equation (3); unless otherwise noted, only experiments within a mass balance of $100 \pm 5\%$ were included in the analysis.

$$MB_{PA}[\%] = \frac{m_{F+uPA} - m_F + m_{F+rPA} - m_F}{m_{PA}} \cdot 100 = \frac{m_{uPA} + m_{rPA}}{m_{PA}} \cdot 100 \quad (3)$$

We acknowledge that drying PA 6 samples at 40 °C at 1 atm does not remove all moisture from the sample but simultaneously found this difference to be small enough to not significantly influence the results.

2.5. Analyses of Recovered PA 6

The calcium content of rPA was measured by dissolving the recovered samples in nitric acid hydrochloride according to DIN EN 13657 (2003-01) and determining the Ca²⁺ content via a complexometric method according to DIN 38406-E3 (2002-03).

The molecular weight distribution was measured according to DIN EN ISO/IEC 17025 by dissolving the polymer in hexafluoroisopropanol (HFIP) and using two gel permeation chromatography (GPC) columns (PSS PSG 100 Å, 7 μm, 8 × 300 mm and PSS PSG 1000 Å, 7 μm, 8 × 300 mm). HFIP was applied as eluent with a flow of $0.7 \frac{\text{mL}}{\text{min}}$. The accuracy of the results was estimated to be within 10%.

2.6. Master Plot Analysis

Master plot analysis is a method of comparing kinetic models with experimental data to obtain information about the reaction mechanism without prior knowledge of the mathematical structure of the rate equation or the kinetic model parameters [28,29]. Detailed discussions of the theoretical foundations of the model equations can be found elsewhere [30,31]. An overview of the solid-state kinetic equations considered in this work is given in Table 2.

Table 2. Solid-state rate expressions for different kinetic models in differential form adapted from Gotor et al. (2000) and Wenzel et al. (2017) [28,29].

Name and Abbreviation	$f(\alpha) = \frac{1}{k} \cdot \frac{d\alpha}{dt}$
1D diffusion (D1)	$(1 - \alpha)^0(1 - (1 - \alpha)^1)^{-1}$
2D diffusion (D2)	$(1 - \alpha)^{1/2}(1 - (1 - \alpha)^{1/2})^{-1}$
3D diffusion (D3)	$(1 - \alpha)^{2/3}(1 - (1 - \alpha)^{1/3})^{-1}$
Reaction order (Fn)	$(1 - \alpha)^n$
Contracting cylinder (R2)	$(1 - \alpha)^{1/2}$
Contracting sphere (R3)	$(1 - \alpha)^{2/3}$
Avrami-Efoeyev (Am)	$m(1 - \alpha)[-log(1 - \alpha)]^{1-1/m}$
Power law (Pn)	α^n

For master plot analysis, a reference point was selected with the dissolution extent $\alpha = 0.5$, and for α between 0 and 1, the value of $\frac{f(\alpha)}{f(0.5)}$ was calculated using the model equations. This allowed the change in dissolution rate over the extent of the dissolution to be compared between different model equations.

The experimental values were incorporated into the master plot by mathematically regressing $Y = f(t)$ and differentiating the obtained correlation equation to calculate the slope of the regression $\frac{d\alpha}{d\theta}$ at the time of each experimental data point, where $\alpha \equiv Y [-]$ describes the dissolution extent and $\theta \equiv t[h]$ is a generalized time. Similar to the model equations, these slopes were compared to the slope at $\alpha = 0.5$, and the resulting value was inserted into the master plot as a marker. Mathematically, this procedure is written as Equation (4), which compares the isothermal experimental data on the left-hand side with the model result on the right-hand side.

$$\frac{\frac{d\alpha}{d\theta}}{\frac{d\alpha}{d\theta}|_{\alpha=0.5}} = \frac{f(\alpha)}{f(0.5)} \quad (4)$$

When the two sides of the equation are approximately equal, the model accurately describes the experimental data points. Thus, a suitable model can be selected graphically without determining the kinetics beforehand.

In this work, the experimental data were regressed to obtain a simple differentiable mathematical function for insertion into Equation (4). No physicochemical meaning was attributed to the numerical values or mathematical structure of the regression functions.

2.7. Experimental Setup to Visualize Ultrasound Enhanced Dissolution

PA filament was extruded using a 3D printer head (Prusa i3 Mk3, Prusa Research, Prague, Czech Republic) to obtain strings with diameters of 150 μm to 250 μm . These extruded strings were held by a 3D-printed structure that was glued to the bottom of a glass cuvette (22.5 \times 25 \times 25 cm^3) and immersed in CEW E; see Figure 3. Sonication was performed using a sonotrode (Sonopuls Ultrasonics homogenizer UW2200, Bandelin, Berlin, Germany) with a 2.0-mm-diameter probe tip. The sonotrode was driven by a linear amplifier (AG1020, Power Conversion Inc., Rochester, NY, USA), which received its signal from a signal generator (DG1022Z, Rigol EU Technologies GmbH, Gilching, Germany), allowing precise control of ultrasound exposure. A LED light source was placed at the back of the sonotrode, and a high-speed camera (FASTCAM Mini AX200, Photron GmbH, Reutlingen, Germany) was placed in front of the sonotrode to record the sonication process.

Topographic surface measurements of the samples were obtained by confocal microscopy. The sample string was removed from the holder after sonication, washed and placed on the measurement platform of the confocal microscope (Marsurf CM Explorer, NanoFocus AG, Oberhausen, Germany). Magnifications between 10 and 50 times were used.

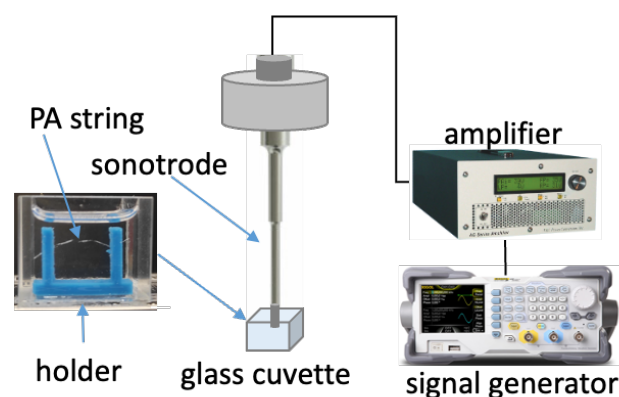


Figure 3. Experimental setup for sonication of the PA string sample. The PA string was held in place by a 3D-printed holder in a glass cuvette. The sonotrode tip on top of the string was driven by an amplifier connected to an external signal generator.

3. Results and Discussion

The details and numeric values of all experiments can be found in the Supplementary Information (S1, S2). The conversion and the yield were always nearly equal and the mass balances were close to 100% for all experiments. Therefore, we conclude that no significant amount of polymer was lost in the process.

3.1. Analyses of Recovered PA 6

Calcium contents above 0.8 wt% have been reported to negatively influence the melt behavior of recovered PA 6.6 [27]. So, the potential accumulation of Ca^{2+} in PA precipitate has to be prevented when designing a PA recycling process with CEW. Therefore, the Ca^{2+} content of the recovered PA was measured for two samples. Values of 0.0037 and 0.0002 wt% were obtained in the recovered samples of the experiments with CEW C and CEW E after 3 h, at 75 °C ultrasonic energy supply with a CEW:PA mass ratio of 8.5 (S5). For reference, the Ca^{2+} content of virgin PA 6 filaments was measured to be 0.004 wt% (S4). Thus, we conclude that our experimental method removes any remaining calcium – introduced from the CEW solvent – sufficiently from the precipitated PA 6 regardless of the applied CEW composition. The amount of water and time of washing are certainly parameters that can be further optimized, drastically lowering the water demand of the process, but they are outside of the scope of this study.

The number and weight average molecular weights (M_n and M_w) and the polydispersity index (PDI) of virgin PA 6 filaments and rPA samples are summarized in Table 3 (S6, S7). No clear trends were observed when the molecular weights of samples from experiments with different CEW compositions or different methods of energy supply under otherwise identical experimental conditions were compared. Although ultrasound has been demonstrated to elevate or diminish the M_n of molten PA 6 (250 °C, 1–2 mm from sonotrode) in previous studies [32,33], we could not observe this effect under our experimental conditions (75 °C, ultrasonic bath). We therefore conclude that the CEW composition and the method of energy supply had no effect on the molecular weight distribution of rPA. If any trend can be made out at all, it is that under otherwise identical experimental conditions, the molecular weights of samples from experiments with longer dissolution times were slightly higher than those of samples from experiments with shorter dissolution times. We attribute this potential increase in molecular weight to a possible appreciable autonomous condensation reaction that even protected against downcycling of the polymer. However, this observation contradicts previous reports that a longer dissolution time leads, if anything, to a decrease in molecular weight [34,35].

Table 3. Number average and weight average molecular weight M_n and M_w as well as polydispersity index (PDI) of virgin PA 6 filaments and recovered PA 6 from experiments with a CEW:PA mass ratio of 8.5 heated at 75 °C.

CEW	Experimental Variables		M_n [10 ⁴ g/mol]	M_w [10 ⁴ g/mol]	PDI [–]
	Energy Supply	Time [h]			
	virgin PA 6 filaments		1.7	3.2	2.0
C	microwave	3	1.4	3.2	2.4
C	microwave	24	1.7	3.6	2.1
E	microwave	3	1.8	3.6	2.0
E	microwave	24	1.8	3.7	2.0
C	ultrasound	3	1.5	3.4	2.3
C	ultrasound	24	1.6	3.6	2.2
E	ultrasound	3	1.3	3.2	2.5
E	ultrasound	24	1.9	3.7	2.0

Ideally, to preserve a polymer's properties, its molecular weight distribution should remain unchanged throughout the dissolution-precipitation cycle. Table 4 summarizes the relative changes in M_n and M_w for dissolution-precipitation processes found in the literature. This change is expressed as the molecular weight of the recovered sample relative to that of the virgin material, with an ideal value being 100%. There is no consensus on a tolerable change. In some studies, values of 64% are considered negligible [36,37], while in other cases, changes beyond 10% are deemed unacceptable [34]. Against this context, we present our measured values, which indicate that PA 6—independently of energy supply, CEW composition or heating time—mostly underwent dissolution rather than chain scission during treatment. This claim is fully in line with the results of Qianhui et al. (2023) [24], who observed no molecular degradation of PA 6 in CEW.

Table 4. Change in molecular weights during dissolution-precipitation of different polymers.

Polymer	M_n	M_w	Change [%]	Reference
PET	M_n		92–98	[38]
PET	M_n		91	[39]
EPS, PS, PVC, PET	M_n		87–99	[40]
PS	M_n		85–100	[41]
PE	M_n		101	[42]
PA 6	M_n		103–104	[22]
PA 6, PA 6.6	M_n		101–105	[19]
PA 4.6	M_n	M_w	93–102	[43]
PA 6		M_w	14–100	[34]
PA 6		M_w	64–94	[37]
PA 6.6		M_w	98–102	[44]
PA 6	M_n	M_w	64–102	[36]
PA 6.6		M_w	100	[45]
PA 6	M_n	M_w	100–107	[24]
PA 6	M_n		78–113	this work
PA 6		M_w	99–117	this work

3.2. Influence of Energy Supply Mode on PA 6 Dissolution

We first investigated the influence of the energy supply mode. Microwave irradiation has been reported to be more energy efficient and faster than conductive heating through direct molecular interactions of the electromagnetic field with the material [46] and was therefore used as the first heating method. Surprisingly, more of the PA 6 filaments dissolved when energy was supplied to the mixture by means of an ultrasonic bath than when energy was supplied by microwaves during a dissolution time of $t \leq 16$ h, as shown in Figure 4. We are the first to report this dissolution enhancement for PA 6 in CEW. For

example, PA 6 recovery increased from 30.7 to 52.2% when energy was introduced into the system via ultrasound rather than microwaves during 5 h of dissolution. In other words, the same amount of PA 6 dissolved more quickly when assisted by ultrasound than when assisted by microwaves. Therefore, ultrasound was selected as the energy supply mode for further investigations. At dissolution times longer than 16 h, the distinctions between the energy supply modes were less pronounced. Further discussion of the comparison of the two modes of energy supply is provided Section 3.4.

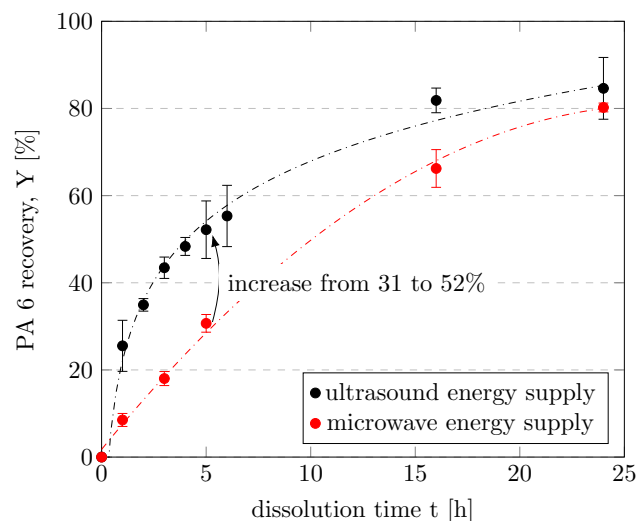


Figure 4. Recovery of PA 6 by energy supply with ultrasound or microwaves as a function of dissolution time. Experiments were performed in a 35-mL vessel with CEW C, a CEW:PA mass ratio of 8.5, and a dissolution temperature of 75 °C.

3.3. Influence of Time on PA 6 Dissolution

Reaction time is a crucial parameter for optimizing space-time-yields, and reducing the dissolution time could greatly reduce costs [47]. We aimed to identify an appropriate time frame for the bulk dissolution of PA 6 to serve as a base case for further investigations.

The recovery of PA 6 as a function of dissolution time is shown in Figure 4. The repeatability of the experiments is indicated by the relative standard deviations, which were largely below 3%. The conversion and recovery of PA 6 increased with increasing dissolution time, which is fully consistent with the results of previous studies [24,25]. A clear trend was observed in which PA 6 recovery increased steeply at short times and gradually leveled off at dissolution times longer than 4 h. In experiments with dissolution times of 72 h, both ultrasound and microwaves resulted in complete dissolution of PA 6. A dissolution time of 3 h was used in subsequent experiments to allow for potential improvements when varying other parameters.

Although we observed complete PA 6 dissolution after 72 h, Rietzler et al. (2018) [25] and Qianhui et al. (2023) [24] reported complete dissolution of PA 6.6 textile fibers or PA 6 textile fibers, respectively, in 2 h or less. This discrepancy is likely due to differences in filament diameter of two orders of magnitude, from several μm (textile fibers) to 1.75 mm (bulk, in this study). Because CEW must penetrate the PA 6 bulk from the outside inward, more time is needed to fully dissolve larger diameter filaments.

3.4. Mechanistic Investigations

The master plots for the various model equations from Table 2 are shown by the lines in Figure 5. For clarity, only one representative mechanism function from each category (Dj, Fn, Ri, Am, Pn) is plotted, although all models were evaluated. For diffusion and

geometrical contraction, the kinetic equations for cylinders (D2, R2) are shown because the pre-cut PA 6 filaments were cylinders.

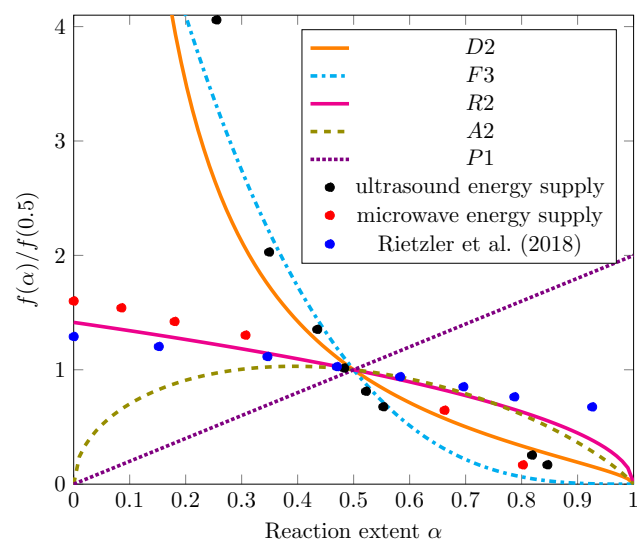


Figure 5. Master plot results with theoretical models as lines according to Table 2 and experimental data as markers. Experiments were performed in 35-mL vessels with CEW C, a CEW:PA mass ratio of 8.5, and a dissolution temperature of 75 °C [25].

The experimental data were regressed as $Y = f(t)$, and the results are displayed in Figure 4. Detailed calculations of the regression functions and their insertion into Equation (4) can be found in the Supplementary Information (S3). For the purposes of comparison with our own work, the values reported by Rietzler et al. (2018) [25] as the change in diameter ΔD were transformed into yield values and regressed as well. All resulting values for $f(\alpha)/f(0.5)$ were added to Figure 5.

A comparison of the experimental values with the model predictions presented in Figure 5 reveals that the values from the microwave energy supply experiments follow a trend that is best described by the model of a contracting cylinder (R2). The likely reason is that the cut PA 6 filaments were cylindrical. In the R2 model, the shrinking reaction interface is the limiting step for the dissolution rate after the initial rapid nucleation on the particle surface [31]. The R2 model also best describes the data measured by Rietzler et al. (2018) [25].

The data from the ultrasonic energy supply experiments (black markers), however, follow a different trend. The dissolution rate is higher at low conversion values and slows dramatically at high conversion values compared with the values obtained in the microwave energy supply experiments. This trend is most accurately described by a diffusion model (D2) or a third-order kinetic model (F3). Under 2D diffusion, the diffusion of Ca^{2+} ions and EtOH into the polymer bulk may be postulated as the rate-limiting mechanism for the dissolution of the PA 6 cylinders. It is similarly conceivable that a product barrier layer of solvated polymer chains—described as the swelling of PA 6.6 fibers by Rietzler et al. (2018) [25]—or a stagnant fluid layer resulting from the absence of stirring inhibits further dissolution [31]. An explanation for a third-order reaction model as the rate-limiting mechanism can be abduced: as proposed by Rietzler et al. (2018) [25] for PA 6.6, the Ca^{2+} ions form a complex with EtOH, breaking down hydrogen bonds, transferring Ca^{2+} to the PA chain, and releasing EtOH. Therefore, all three components (CaCl_2 , EtOH, and amide) may contribute to dissolution, leading to third-order reaction kinetic behavior. At this stage, we cannot make any specific conclusion on the dissolution mechanism.

The key aspect to be clarified is why the ultrasound data show a different overall mechanistic trend than the microwave data. We rationalize this observation with the follow-

ing hypothesis that discriminates the rate of diffusion of CEW into the PA particles (k_{dif}) from the rate of PA 6 chain disentanglement into CEW (k_{dis}), which together contribute to the overall observed rate k_{obs} according to Equation (5):

$$\frac{1}{k_{obs}} = \frac{1}{k_{dif}} + \frac{1}{k_{dis}} \quad (5)$$

In the case of energy supply from microwaves, k_{dif} is high due to stirring, but k_{dis} is much lower than in the case of ultrasonic energy supply. Consequently, dissolution is the rate-determining step, resulting in the observed mechanism (R2), which is consistent with the literature [48]. In the case of ultrasonic energy supply, k_{dif} is low, but k_{dis} is high compared with energy supply from microwaves. This results in a mechanism where the diffusion (D2) or the reaction rate (F3) determines the observed rate. This reasoning could explain the observed difference in mechanism and is simultaneously compatible with the observation that the dissolution of PA 6 in CEW clearly proceeds faster when energy is supplied by ultrasound than by microwaves for $t < 16$ h (see Figure 4). Rapid heating as provided by microwaves and stirring hence does not seem to be as important for the overall dissolution rate of PA 6 filaments in CEW as the effective mass transfer promoted by ultrasound. The formulated hypothesis is in line with the literature for other polymers [8,47–49] and will be subject to further investigations in our laboratory.

3.5. Surface Structure of Sonicated PA Strings

To further understand the effect of ultrasound on the dissolution of polyamide, we conducted microscopic experiments that, to some extent, resembled the treatment in the ultrasonic bath. Details on the results of these visualizations can be found in the Supplementary Information (S8). The application of ultrasound generates stable cavitation bubbles [50], which oscillate around and on the PA strings and remain attached to the strings due to hydrophobic interactions, as shown in Figure 6. These bubbles seem to be responsible for the enhanced dissolution, as they act as local micro-mixers that enhance local mass transfer. This may be the reason why k_{dis} is higher when energy is supplied by ultrasound than when energy is supplied by microwaves.

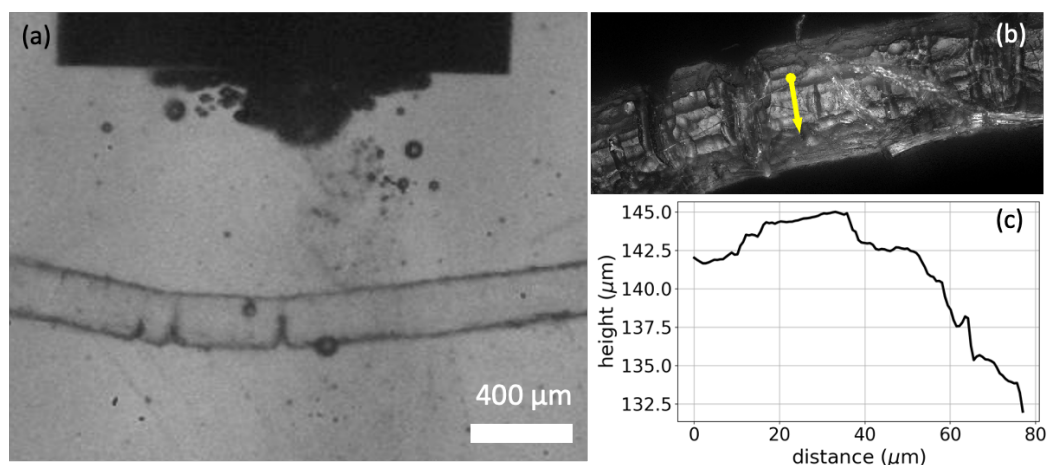


Figure 6. (a) Multiple bubbles appear and oscillate on the PA string during sonication. (b) 20× magnification image of the string near the ultrasound focal volume. Deep trenches are observed on the surface of the string. (c) Rough surface profile of the string as measured along the yellow arrow of (b).

3.6. Influence of CEW Composition on PA 6 Dissolution

In Figure 7, the compositions of the applied CEW mixtures (see Table 1) are displayed on a ternary diagram. CEW G did not dissolve the PA 6 filaments. CEWs A, B, C, D and E contributed to substantial dissolution of PA 6. When CEW F was used, the filaments agglomerated into one solid piece during the experiment, drastically altering their surface area. Hence, we did not pursue further experiments with CEW F. Furthermore, the PA 6 filaments floated on top of CEWs F and G. These CEW mixtures have high H₂O:EtOH molar ratios, and we attribute the floating of the filaments to the high density of these mixtures compared with the density of the PA filaments. Our observations are consistent with the findings of Rietzler et al. (2018) [25] on PA 6.6 dissolution in CEW, which indicated that the dissolution process is influenced by solvent composition. In Figure 7, the blue and orange boxes mark the ternary compositions for swelling and dissolution of PA 6.6 taken from Rietzler et al. (2018) [25] for reference. The red dot in Figure 7 shows the composition obtained after adding the antisolvent. This composition falls within the region where no dissolution of PA 6 filaments or PA 6.6 fibers was observed and therefore all dissolved PA precipitated from the solution.

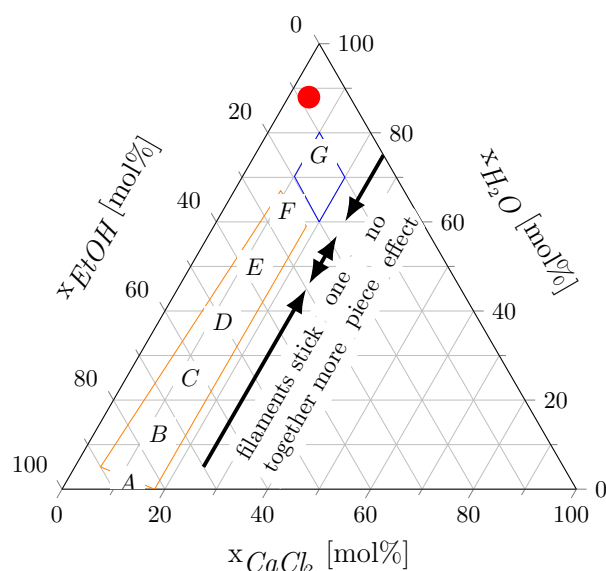


Figure 7. Ternary diagram of the CaCl₂-EtOH-H₂O-system for PA 6 dissolution. The letters indicate the CEW compositions from Table 1, the arrows describe how the PA filaments agglomerated in CEW, and the red dot marks the composition obtained after adding the antisolvent. The orange and blue boxes mark the dissolution and swelling compositions for PA 6.6 reported by Rietzler et al. (2018) [25].

Figure 8 illustrates the quantitative influence of the H₂O:EtOH molar ratio on PA 6 recovery. CEWs A, B, D and E dissolved significantly more PA than CEW C. This was surprising to us since we expected CEW with a low H₂O:EtOH molar ratio to dissolve more PA 6 due to the complex formation of Ca²⁺ with EtOH described in Section 3.4. Further specific investigations are needed to fully understand the interplay of CEW with different H₂O:EtOH molar ratios with PA 6, possibly also considering water solvating the Ca²⁺ and simultaneously acting as an antisolvent for PA 6.

Although the experiments using CEW E often had to be repeated due to inaccuracies in the mass balances and agglomeration of the undissolved filaments, CEW E clearly gave the highest average recovery of PA 6. This result justified its selection for further investigations. The dissolution behaviors of PA 6 and PA 6.6 might differ, as Rietzler et al. (2018) [25] reported—albeit without further clarification—that CEW C was the best mixture for dissolving PA 6.6 fibers, and Qianhui et al. (2023) [24] used only CEW C to dissolve PA 6.

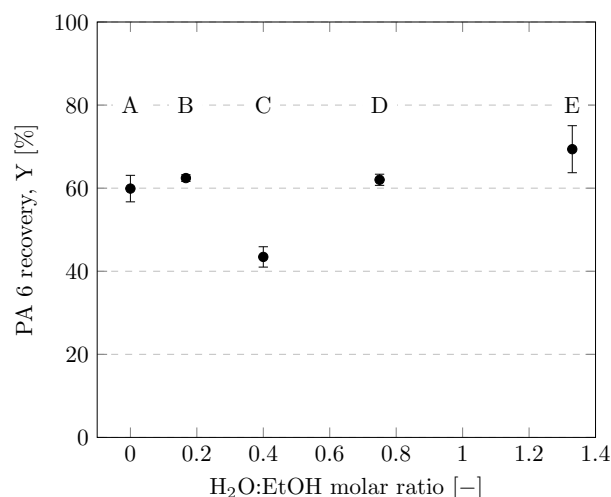


Figure 8. Recoveries of PA 6 using various CEW compositions according to Table 1. Experiments were performed in 35-mL vessels with a CEW:PA mass ratio of 8.5 and heating with ultrasound at a dissolution temperature of 75 °C for 3 h.

3.7. Influence of CEW:PA Mass Ratio

The solvent-to-feed ratio is an important parameter for designing and scaling-up a process [47,51]. In general, the use of solvents is minimized due to their cost, which allows for the use of smaller reactors and separation units in downstream processing [16]. However, very low solvent-to-feed ratios can cause solubility problems for solid reactants. The effects of CEW:PA mass ratios between 4 and 30 are depicted in Figure 9. For CEW:PA mass ratios of 4 and 5, the mass balances were slightly outside of the 5% deviation range, and significantly less PA was dissolved compared with a CEW:PA mass ratio of 8.5. Nevertheless, no significant improvement in dissolution was observed at CEW:PA mass ratios above 8.5 (error bars overlap). A likely explanation for this observation is that filament agglomeration increases at CEW:PA mass ratios below 8.5 and that CEW cannot penetrate into the agglomerates. By contrast, at CEW:PA mass ratios ≥ 8.5 , the filaments were dispersed in an excess of solvent, facilitating their dissolution. Thus, a CEW:PA mass ratio of 8.5 is a highly rational value.

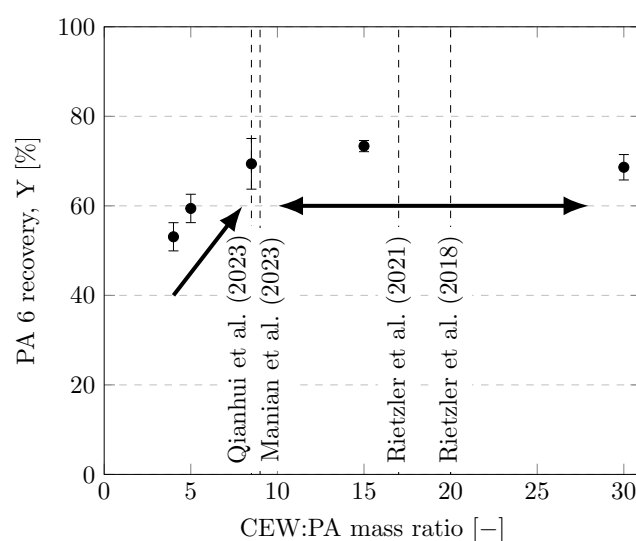


Figure 9. Recoveries of PA 6 at different CEW:PA mass ratios. Experiments were performed in 35-mL vessels (100 mL for CEW:PA ≥ 15) with CEW E heated with an ultrasonic bath at a dissolution temperature of 75 °C for 3 h. Values used in the literature are given as dashed lines [24–27].

4. Conclusions and Outlook

In this work, we report the first investigations of the dissolution of bulk PA 6 in CEW. A critical implication of our work is that CEW can be used to recycle not only small fibres but also larger particles such as shredded PA 6 pieces or composite materials containing PA 6 from mixed plastics waste. Thus, our study expands the use cases for solvent-based recycling for a resource-intensive polymers such as PA 6. Supplying energy by ultrasound was more effective than supplying energy by microwaves; the former improved the yield of dissolved and recovered PA 6 after 5 h from 31% to 52%. Moreover, the H₂O:EtOH molar ratio was a pivotal determinant of the dissolution efficiency of PA 6. CEW:PA ratios ≥ 8.5 were necessary to promote swift dissolution in excess solvent. Overall, we found that the yield of rPA after 3 h of bulk dissolution at a CEW:PA mass ratio of 8.5 increased from 18% to 69% when the energy supply mode was changed from microwaves to ultrasound and the CEW mixture from CEW C to CEW E.

The analyses of rPA demonstrated that any remaining solvent impurities were sufficiently removed. The CEW composition and method of energy supply during dissolution had no distinct effects on the molecular mass distribution of PA 6, whereas increasing the dissolution time slightly increased the molecular mass of PA 6. In alignment with results in the literature on dissolution-precipitation processes, we found that with our experimental method, PA 6 underwent dissolution rather than degradation through amide bond hydrolysis.

Our study is the first to report mass recoveries and mass balances alongside mass conversions for the dissolution of PA using CEW. Our data allowed us to close the mass balances for PA 6 and show that no significant amount of polymer was lost in the process. Therefore, a crucial requirement for circular economy of closing the loop and not losing polymer to the environment or to side reactions is also met.

Additionally, we explored the potential mechanisms of PA 6 dissolution in CEW. Master plot analysis indicated that microwave-assisted dissolution followed a contracting cylinder model, whereas ultrasound-assisted dissolution aligned with a 2D diffusion or third-order kinetic model. Our microscopic observations suggested that in the case of ultrasonic energy supply, the dissolution rate was enhanced by oscillating bubbles on the particle surface.

In future research, we will conduct more precise assessments of kinetic behavior and alter important dissolution parameters, including dissolution temperature and pH. Further research will have to answer the question, whether ultrasound is also beneficial for dissolving PA 6 samples containing dirt, other polymers, fillers, colorants, stabilizers, flame retardants, plasticizers etc. Furthermore, investigating the impact of precipitation and separation parameters will provide valuable insights into the development of a large-scale process. Next, we aim to develop a computational model for an industrial-scale PA 6 dissolution process, which preferably should provide insights into the economic and environmental potential of the proposed separation/recycling approach.

Supplementary Materials: The following supporting information can be downloaded at: <https://www.mdpi.com/article/10.3390/recycling10010005/s1>.

Author Contributions: Conceptualization, R.G., A.-J.M., L.R.-S. and K.S.; Data curation, R.G. and L.R.-S.; Formal analysis, R.G. and C.-D.O.; Funding acquisition, K.S.; Investigation, R.G., P.P. and S.-W.O.; Methodology, R.G.; Resources, K.S. and C.-D.O.; Supervision, L.R.-S. and K.S.; Visualization, R.G.; Writing—original draft, R.G. and S.-W.O.; Writing—review and editing, R.G., A.-J.M., L.R.-S., S.-W.O., P.P., C.-D.O. and K.S. All authors have read and agreed to the published version of the manuscript.

Funding: This work was supported by the Research Initiative SmartProSys funded by the Ministry for Science, Energy, Climate Protection and Environment of the State of Saxony-Anhalt, Germany.

In addition, we thank the Supporting Members of the Max Planck Society for their donations to MaxDePoly research project.

Data Availability Statement: The original contributions presented in the study are included in the article and supplementary material, further inquiries can be directed to the corresponding author.

Acknowledgments: The authors gratefully acknowledge our colleagues Jins Philip Jacob, Bianka Stein, Shikha Gupta, Dimana Karabozhilova and Katja Guttmann for their support in performing and analyzing the experiments.

Conflicts of Interest: The funders had no role in the design of the study; in the collection, analyses, or interpretation of data; in the writing of the manuscript; or in the decision to publish the results.

References

1. McGlade, C.; Ekins, P. The geographical distribution of fossil fuels unused when limiting global warming to 2 °C. *Nature* **2015**, *517*, 187–190. [CrossRef] [PubMed]
2. Masson-Delmotte, V.; Zhai, P.; Pörtner, H.O.; Roberts, D.; Skea, J.; Shukla, P.R.; Pirani, A.; Moufouma-Okia, W.; Péan, C.; Pidcock, R.; et al. *Global Warming of 1.5 °C. An IPCC Special Report on the Impacts of Global Warming of 1.5 °C Above Pre-Industrial Levels and Related Global Greenhouse Gas Emission Pathways, in the Context of Strengthening the Global Response to the Threat of Climate Change, Sustainable Development, and Efforts to Eradicate Poverty*; Cambridge University Press: Cambridge, UK; New York, NY, USA, 2018; p. 616. [CrossRef]
3. Geyer, R.; Jambeck, J.R.; Law, K.L. Production, use, and fate of all plastics ever made. *Sci. Adv.* **2017**, *3*, e1700782. [CrossRef] [PubMed]
4. MacArthur Foundation, E. Towards the circular economy. *J. Ind. Ecol.* **2013**, *2*, 23–44.
5. van den Beuken, E.; Urbanus, J.H.; Stegmann, P.; van Harmelen MSc, T.; Ligthart, T.; Bertling, D.I.J.; Kabasci, I.S.; Renner, I.M. From #plasticfree to Future-Proof Plastics. 2023. Available online: <https://www.umsicht.fraunhofer.de/content/dam/umsicht/en/documents/publications/2023/White-paper-From-plasticfree-to-future-proof-plastics.pdf> (accessed on 23 May 2023).
6. Hopewell, J.; Dvorak, R.; Kosior, E. Plastics recycling: Challenges and opportunities. *Philos. Trans. R. Soc. B Biol. Sci.* **2009**, *364*, 2115–2126. [CrossRef] [PubMed]
7. Rahimi, A.; García, J.M. Chemical recycling of waste plastics for new materials production. *Nat. Rev. Chem.* **2017**, *1*, 0046. [CrossRef]
8. Zhao, Y.B.; Lv, X.D.; Ni, H.G. Solvent-based separation and recycling of waste plastics: A review. *Chemosphere* **2018**, *209*, 707–720. [CrossRef]
9. Tonsi, G.; Maesani, C.; Alini, S.; Ortenzi, M.A.; Pirola, C. Nylon Recycling Processes: A Brief Overview. *Chem. Eng. Trans.* **2023**, *100*, 727–732. [CrossRef]
10. Lange, J.P. Sustainable development: Efficiency and recycling in chemicals manufacturing. *Green Chem.* **2002**, *4*, 546–550. [CrossRef]
11. Hirschberg, V.; Rodrigue, D. Recycling of polyamides: Processes and conditions. *J. Polym. Sci.* **2023**, *61*, 1937–1958. [CrossRef]
12. Ben Amor, I.; Klinkova, O.; Baklouti, M.; Elleuch, R.; Tawfiq, I. Mechanical Recycling and Its Effects on the Physical and Mechanical Properties of Polyamides. *Polymers* **2023**, *15*, 4561. [CrossRef] [PubMed]
13. Minor, A.J.; Goldhahn, R.; Rihko-Struckmann, L.; Sundmacher, K. Chemical Recycling Processes of Nylon 6 to Caprolactam: Review and Techno-Economic Assessment. *Chem. Eng. J.* **2023**, *474*, 145333. [CrossRef]
14. Vollmer, I.; Jenks, M.J.; Roelands, M.C.; White, R.J.; Van Harmelen, T.; De Wild, P.; van Der Laan, G.P.; Meirer, F.; Keurentjes, J.T.; Weckhuysen, B.M. Beyond mechanical recycling: Giving new life to plastic waste. *Angew. Chem. Int. Ed.* **2020**, *59*, 15402–15423. [CrossRef] [PubMed]
15. Arena, U.; Ardolino, F. Technical and environmental performances of alternative treatments for challenging plastics waste. *Resour. Conserv. Recycl.* **2022**, *183*, 106379. [CrossRef]
16. Mangold, H.; von Vacano, B. The frontier of plastics recycling: rethinking waste as a resource for high-value applications. *Macromol. Chem. Phys.* **2022**, *223*, 2100488. [CrossRef]
17. Raju, K.; Yaseen, M. Influence of nonsolvents on dissolution characteristics of nylon-6. *J. Appl. Polym. Sci.* **1991**, *43*, 1533–1538. [CrossRef]
18. Zagouras, N.; Koutinas, A. Processing scheme based on selective dissolution to recycle food packaging and other polymeric wastes and its economic analysis. *Waste Manag. Res.* **1995**, *13*, 325–333. [CrossRef]
19. Kartalis, C.; Poulakis, J.; Tsenoglou, C.; Papaspyrides, C. Pure component recovery from polyamide 6/6 mixtures by selective dissolution and reprecipitation. *J. Appl. Polym. Sci.* **2002**, *86*, 1924–1930. [CrossRef]

20. Busquets-Fité, M.; Fernandez, E.; Janer, G.; Vilar, G.; Vázquez-Campos, S.; Zanasca, R.; Citterio, C.; Mercante, L.; Puentes, V. Exploring release and recovery of nanomaterials from commercial polymeric nanocomposites. *J. Phys. Conf. Ser.* **2013**, *429*, 012048. [[CrossRef](#)]
21. Costamagna, M.; Massaccesi, B.M.; Mazzucco, D.; Baricco, M.; Rizzi, P. Environmental assessment of the recycling process for polyamides-Polyethylene multilayer packaging films. *Sustain. Mater. Technol.* **2023**, *35*, e00562. [[CrossRef](#)]
22. Papaspyrides, C.; Kartalis, C. A model study for the recovery of polyamides using the dissolution/precipitation technique. *Polym. Eng. Sci.* **2000**, *40*, 979–984. [[CrossRef](#)]
23. Önal, M.A.R.; Dewilde, S.; Degri, M.; Pickering, L.; Saje, B.; Riaño, S.; Walton, A.; Binnemans, K. Recycling of bonded NdFeB permanent magnets using ionic liquids. *Green Chem.* **2020**, *22*, 2821–2830. [[CrossRef](#)]
24. Xu, Q.; Hu, H.; Zhu, R.; Sun, L.; Yu, J.; Wang, X. A non-destructive, environment-friendly method for separating and recycling polyamide 6 from waste and scrap polyamide 6 blended textiles. *Text. Res. J.* **2023**, *93*, 3327–3340. [[CrossRef](#)]
25. Rietzler, B.; Bechtold, T.; Pham, T. Controlled surface modification of polyamide 6.6 fibres using CaCl₂/H₂O/EtOH solutions. *Polymers* **2018**, *10*, 207. [[CrossRef](#)]
26. Rietzler, B.; Manian, A.P.; Rhomberg, D.; Bechtold, T.; Pham, T. Investigation of the decomplexation of polyamide/CaCl₂ complex toward a green, nondestructive recovery of polyamide from textile waste. *J. Appl. Polym. Sci.* **2021**, *138*, 51170. [[CrossRef](#)]
27. Manian, A.P.; Kraegeloh, F.E.; Braun, D.E.; Mahmud-Ali, A.; Bechtold, T.; Pham, T. Separation of polyamide 66 from mixtures with cellulose fibers by selective dissolution in calcium chloride-ethanol-water solvent. *J. Appl. Polym. Sci.* **2023**, *140*, e53813. [[CrossRef](#)]
28. Gotor, F.J.; Criado, J.M.; Malek, J.; Koga, N. Kinetic analysis of solid-state reactions: The universality of master plots for analyzing isothermal and nonisothermal experiments. *J. Phys. Chem. A* **2000**, *104*, 10777–10782. [[CrossRef](#)]
29. Wenzel, M.; Dharanipragada, N.A.; Galvita, V.V.; Poelman, H.; Marin, G.B.; Rihko-Struckmann, L.; Sundmacher, K. CO production from CO₂ via reverse water–gas shift reaction performed in a chemical looping mode: Kinetics on modified iron oxide. *J. CO₂ Util.* **2017**, *17*, 60–68. [[CrossRef](#)]
30. Vyazovkin, S.; Wight, C. Kinetics in solids. *Annu. Rev. Phys. Chem.* **1997**, *48*, 125–149. [[CrossRef](#)]
31. Khawam, A.; Flanagan, D.R. Solid-state kinetic models: Basics and mathematical fundamentals. *J. Phys. Chem. B* **2006**, *110*, 17315–17328. [[CrossRef](#)] [[PubMed](#)]
32. Li, J.; Liang, M.; Guo, S.; Lin, Y. Studies on chain scission and extension of polyamide 6 melt in the presence of ultrasonic irradiation. *Polym. Degrad. Stab.* **2004**, *86*, 323–329. [[CrossRef](#)]
33. Lin, H.; Isayev, A. Ultrasonic treatment of polypropylene, polyamide 6, and their blends. *J. Appl. Polym. Sci.* **2006**, *102*, 2643–2653. [[CrossRef](#)]
34. Wang, Z.L.; Xu, J.L.; Wu, L.J.; Chen, X.; Yang, S.G.; Liu, H.C.; Zhou, X.J. Dissolution, hydrolysis and crystallization behavior of polyamide 6 in superheated water. *Chin. J. Polym. Sci.* **2015**, *33*, 1334–1343. [[CrossRef](#)]
35. Mohod, A.V.; Gogate, P.R. Ultrasonic degradation of polymers: Effect of operating parameters and intensification using additives for carboxymethyl cellulose (CMC) and polyvinyl alcohol (PVA). *Ultrason. Sonochem.* **2011**, *18*, 727–734. [[CrossRef](#)] [[PubMed](#)]
36. Gardeniers, M.; Mani, M.; de Boer, E.; Hermida-Merino, D.; Graf, R.; Rastogi, S.; Harings, J.A. Hydration, refinement, and dissolution of the crystalline phase in polyamide 6 polymorphs for ultimate thermomechanical properties. *Macromolecules* **2022**, *55*, 5080–5093. [[CrossRef](#)] [[PubMed](#)]
37. Knappich, F.; Klotz, M.; Schlummer, M.; Wölling, J.; Mäurer, A. Recycling process for carbon fiber reinforced plastics with polyamide 6, polyurethane and epoxy matrix by gentle solvent treatment. *Waste Manag.* **2019**, *85*, 73–81. [[CrossRef](#)]
38. Poulakis, J.; Papaspyrides, C. Dissolution/precipitation: A model process for PET bottle recycling. *J. Appl. Polym. Sci.* **2001**, *81*, 91–95. [[CrossRef](#)]
39. Chen, W.; Yang, Y.; Lan, X.; Zhang, B.; Zhang, X.; Mu, T. Biomass-derived γ -valerolactone: Efficient dissolution and accelerated alkaline hydrolysis of polyethylene terephthalate. *Green Chem.* **2021**, *23*, 4065–4073. [[CrossRef](#)]
40. Achilias, D.; Giannoulis, A.; Papageorgiou, G. Recycling of polymers from plastic packaging materials using the dissolution–precipitation technique. *Polym. Bull.* **2009**, *63*, 449–465. [[CrossRef](#)]
41. García, M.T.; Gracia, I.; Duque, G.; De Lucas, A.; Rodríguez, J.F. Study of the solubility and stability of polystyrene wastes in a dissolution recycling process. *Waste Manag.* **2009**, *29*, 1814–1818. [[CrossRef](#)]
42. Poulakis, J.; Papaspyrides, C. The dissolution/precipitation technique applied on high-density polyethylene: I. Model recycling experiments. *Adv. Polym. Technol. J. Polym. Process. Inst.* **1995**, *14*, 237–242. [[CrossRef](#)]
43. Deshmukh, Y.S.; Graf, R.; Hansen, M.R.; Rastogi, S. Dissolution and crystallization of polyamides in superheated water and concentrated ionic solutions. *Macromolecules* **2013**, *46*, 7086–7096. [[CrossRef](#)]
44. Mu, B.; Yang, Y. Complete separation of colorants from polymeric materials for cost-effective recycling of waste textiles. *Chem. Eng. J.* **2022**, *427*, 131570. [[CrossRef](#)]

45. Mu, B.; Shao, Y.; Yu, X.; McBride, L.; Hidalgo, H.; Yang, Y. High-quality separation and recovery of nylon and dyes from waste carpet via non-destructive dissolution and controlled precipitation for sustainable recycling. *Sep. Purif. Technol.* **2024**, *332*, 125801. [[CrossRef](#)]
46. Sun, J.; Wang, W.; Yue, Q. Review on microwave-matter interaction fundamentals and efficient microwave-associated heating strategies. *Materials* **2016**, *9*, 231. [[CrossRef](#)] [[PubMed](#)]
47. Vandenburg, H.; Clifford, A.; Bartle, K.; Garden, L.; Dean, J.; Costley, C. Critical review: Analytical extraction of additives from polymers. *Analyst* **1997**, *122*, 101R–116R. [[CrossRef](#)]
48. Miller-Chou, B.A.; Koenig, J.L. A review of polymer dissolution. *Prog. Polym. Sci.* **2003**, *28*, 1223–1270. [[CrossRef](#)]
49. Stamatialis, D.; Sanopoulou, M.; Raptis, I. Swelling and dissolution behavior of poly (methyl methacrylate) films in methyl ethyl ketone/methyl alcohol mixtures studied by optical techniques. *J. Appl. Polym. Sci.* **2002**, *83*, 2823–2834. [[CrossRef](#)]
50. Leighton, T. *The Acoustic Bubble*; Academic Press: London, UK; San Diego, CA, USA, 2012; pp. 341–430.
51. Martínez, J.; Sales Silva, L.P. Scale-up of Extraction Processes. In *Natural Product Extraction: Principles and Applications*; The Royal Society of Chemistry: London, UK, 2013; pp. 363–398. [[CrossRef](#)]

Disclaimer/Publisher’s Note: The statements, opinions and data contained in all publications are solely those of the individual author(s) and contributor(s) and not of MDPI and/or the editor(s). MDPI and/or the editor(s) disclaim responsibility for any injury to people or property resulting from any ideas, methods, instructions or products referred to in the content.